J. Fluid Mech. (1981), *vol.* 113, *pp.* 221–239
Printed in Great Britain

Viscous fluid buckling of plane and axisymmetric jets

By J. O. CRUICKSHANK AND B. R. MUNSON
Department of Engineering Science and Mechanics, and Engineering Research Institute, Iowa State University, Ames, Iowa 50011

(Received 11 August 1980 and in revised form 16 March 1981)

Experimental results are presented concerning the spontaneous oscillations observed when a high-viscosity fluid jet flows vertically against a flat surface. The two jet shapes investigated were the axisymmetric jet and the plane jet. The minimum distance from the jet orifice to the flat surface for which these oscillations are observed, termed the 'buckling height', was determined experimentally. The frequency of the subsequent oscillations was also determined. Both were measured as functions of fluid and flow variables. It is found that surface tension effects are the dominant factors influencing the buckling height, while the rate of oscillation is affected by both surface tension effects and by viscous, gravity and inertia effects. The major results are presented in non-dimensional form. Photographs of the buckling phenomenon are provided for representative jet geometries. It is also established experimentally that there is an upper limit to the flow Reynolds number above which buckling does not occur.

1. Introduction

In numerous areas of solid mechanics, the concept of buckling is an important and fairly well-understood phenomenon. The understanding of the buckling of columns, beams, plates and other structures is critical in many design situations. The phenomenon of buckling, i.e. the transition from the straight to the bent configuration at the buckling load, occurs because the straight configuration ceases to be stable. The buckling of structures has been extensively investigated, both theoretically and experimentally. For example, the well-known Euler equations govern the critical load for elastic buckling in slender columns with given end conditions.

Within the realm of fluid mechanics, a similar phenomenon is observed – a phenomenon typified by the familiar coiling of a thin stream of honey as it falls onto a flat plate. Careful observations indicate that a high-viscosity fluid such as honey may depart spontaneously from a stable axially symmetric stagnation jet flow and, under the appropriate physical conditions, maintain a state in which oscillations in the form of coiling or folding are observed in that region of the jet close to the stagnation surface. Typical situations illustrating this are shown in figures 1–5. This spontaneous transition from a condition of steady, stable flow to unsteady oscillations of parts of the jet column we refer to as 'fluid buckling', in analogy with its much studied counterpart in solid mechanics.

As indicated in figure 1, if the distance H between the orifice and the flat plate against which the viscous jet flows is less than the critical value H_c, the jet will be stable. For $H > H_c$, the jet is unstable and will buckle. Such fluid buckling has received

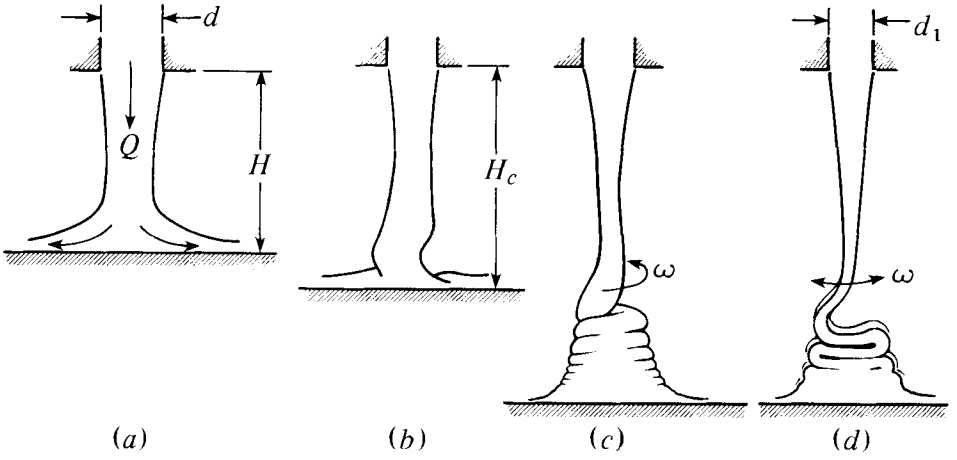

FIGURE 1. Nomenclature for fluid buckling of a viscous jet. (*a*) Stable, unbuckled jet; (*b*) buckling begins at critical height; (*c*) buckled axisymmetric jet (coiling); (*d*) buckled plane jet (folding).

very little attention since it was first investigated qualitatively by Taylor (1968). Lienhard (1968) has presented experimental results concerning a somewhat related instability of small, low-viscosity (water) jets impinging on a surface. Suleiman & Munson (1981) have studied a related phenomenon, the buckling of thin layers of very viscous liquids subjected to shear flow; this type of fluid buckling corresponds to the buckling of solid plates under the application of a shear force loading.

Physically, the reason for the buckling of a viscous jet can be attributed to the fact that a viscous jet may be either in tension or compression, depending on the velocity gradient along its axis (Cruickshank 1980). If the dimaeter of the jet increases in the downstream direction, the viscous normal stress along its axis is one of compression. If this viscous compressive component of the normal stress is large enough, the net axial stress in the jet (including the tensile effect of the surface tension contribution) may be compressive. Thus, near the flat plate, sufficiently large axial compressive stresses along with a sufficiently 'slender' jet combine, under appropriate circumstances, to produce the fluid mechanics analogue to the buckling of a slender solid column.

The purpose of the present paper is to present extensive experimental results to quantify the instability that results in the buckling of a viscous jet that flows against a flat plate. The important dimensionless parameters are identified and their values for the critical buckling and post-buckled flows are determined.

2. Dimensional analysis of the fluid buckling process

As indicated in the previous section, a very viscous jet impinging upon a flat surface may become unstable and buckle if its length becomes too large. As seen in figures 2–5 this buckling may occur for jets of various cross-sectional shapes. For the majority of our experimental investigation, we used two basic shapes – the round axisymmetric jet (circular orifice) and the plane jet (slot orifice). The important dimensionless parameters associated with the buckling process for these jets can be obtained as indicated below.

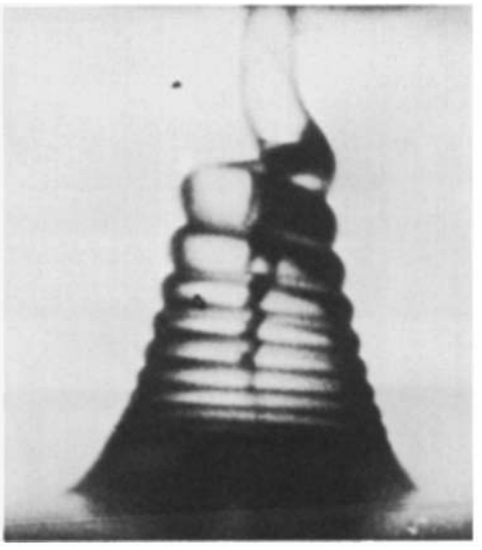

(*a*)

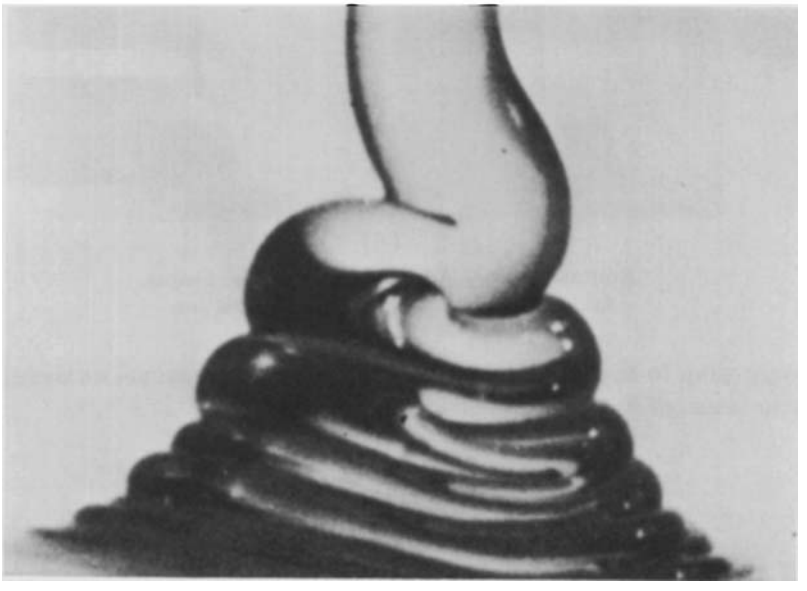

(*b*)

FIGURE 2. Buckled axisymmetric jet. (*a*) Coiling: $H = 1{\cdot}98$ cm, $Q = 9{\cdot}74 \times 10^{-2}$ cm^3/s, $d = 0{\cdot}114$ cm, $\omega = 55$ Hz, $\nu = 5500$ cSt; (*b*) folding: $H = 9{\cdot}1$ cm, $Q = 20{\cdot}7$ cm^3/s, $d = 1{\cdot}27$ cm, $\omega = 9{\cdot}67$ Hz, $\nu = 5500$ cSt.

It is postulated that the frequency of oscillation of the buckled axisymmetric jet ω depends on the following variables:

$$\omega = \omega(H, g, d, Q, \sigma, \rho, \mu), \tag{1}$$

where H is the distance from the orifice to the flat surface, g is the acceleration due to gravity, d is the diameter of jet orifice, Q is the volume flow rate of fluid, and σ, ρ, and μ are the fluid surface tension, density, and viscosity, respectively.

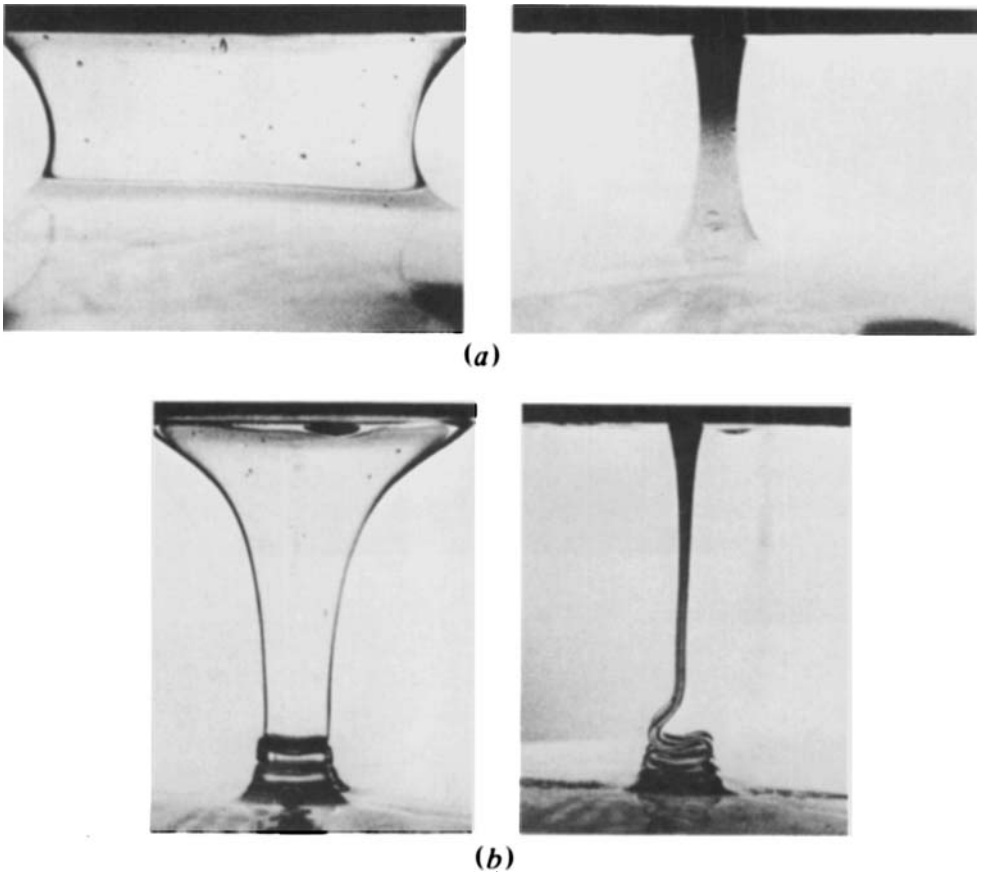

FIGURE 3. Buckling of a plane jet. (*a*) Stable, unbuckled jet; (*b*) unstable, buckled jet.

Thus, according to the Buckingham Pi theorem of dimensional analysis, (1) can be rewritten in terms of five non-dimensional groups:

$$\omega(d/g)^{\frac{1}{2}} = F_1\left(\frac{\sigma}{\gamma d^2}, \frac{\mu Q}{\gamma d^4}, \frac{gd^3}{\nu^2}, \frac{H}{d}\right), \tag{2}$$

where $\nu = \mu/\rho$ and $\gamma = \rho g$ are the kinematic viscosity and the specific weight, respectively.

According to this non-dimensional representation, the dimensionless frequency of oscillation $\omega(d/g)^{\frac{1}{2}}$ is a function of four parameters: (1) the ratio of surface tension forces to gravitational forces $\sigma/\gamma d^2$, (2) the ratio of viscous forces to gravitational forces $\mu Q/\gamma d^4$, (3) the ratio of inertia forces times gravity forces to viscous forces gd^3/ν^2, and (4) the slenderness ratio H/d.

For $H < H_c$ the jet is stable, ω does not exist (no oscillations) so that the critical length-to-diameter ratio may be written as

$$\frac{H_c}{d} = F_2\left(\frac{\sigma}{\gamma d^2}, \frac{\mu Q}{\gamma d^4}, \frac{gd^3}{\nu^2}\right). \tag{3}$$

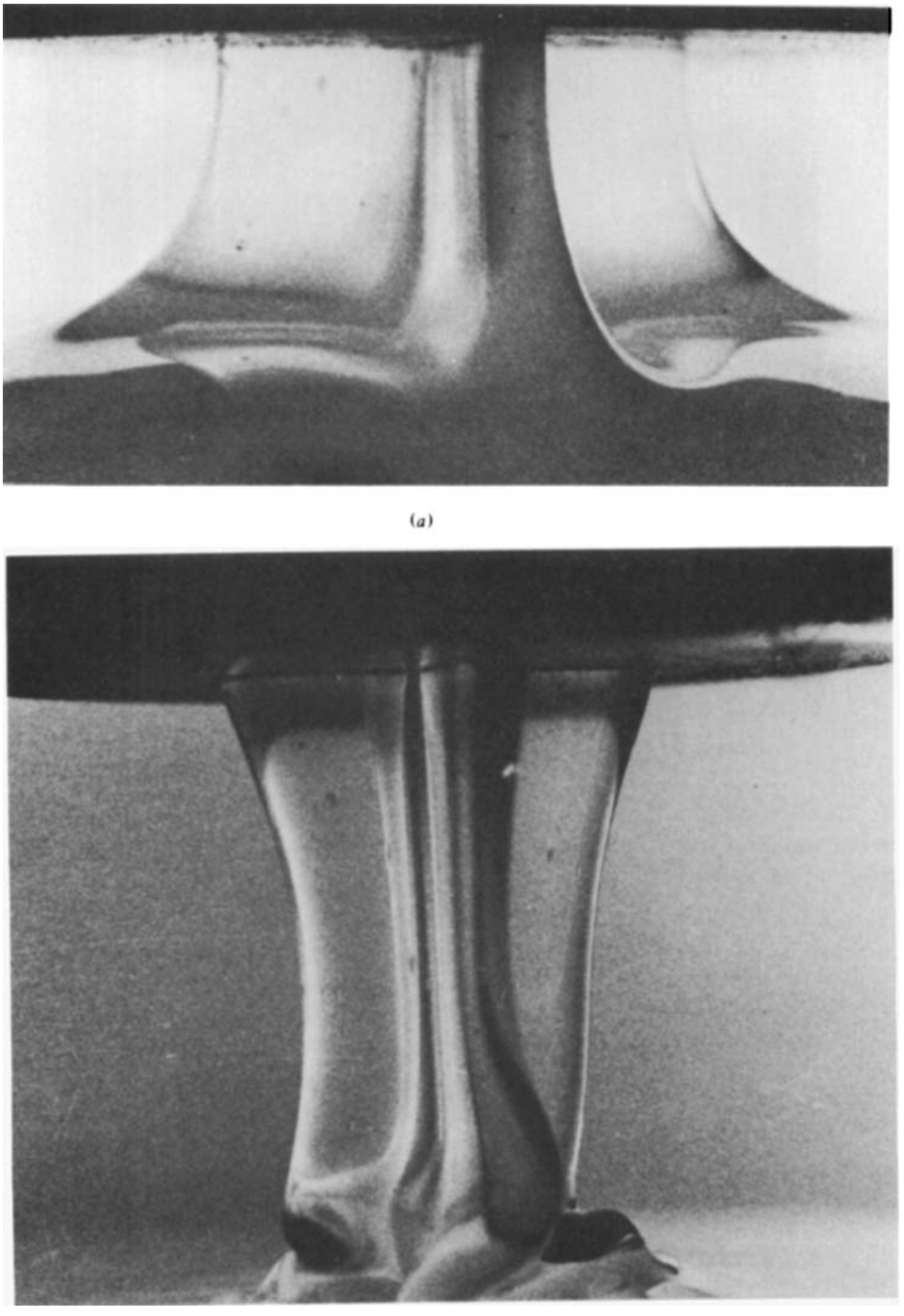

(*a*)

(*b*)

FIGURE 4. Buckling of an X-shaped jet. (*a*) Stable, unbuckled; (*b*) unstable, buckled.

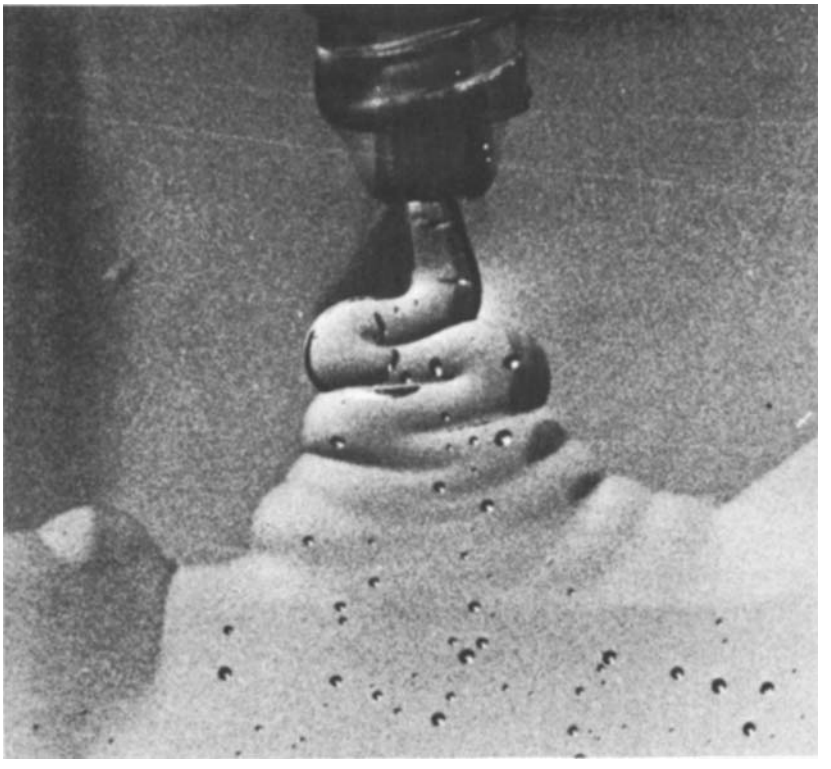

FIGURE 5. Buckling of a jet of 10000 cSt oil floating on water.

We further assume that the buckling process itself is a low-Reynolds-number phenomenon, implying that inertia effects are negligible; thus, the only term involving density ($gd^3/\nu^2 = \rho^2 gd^3/\mu^2$) may be neglected. Hence, (3) may be rewritten as

$$\frac{H_c}{d} = F_3\left(\frac{\sigma}{\gamma d^2}, \frac{\mu Q}{\gamma d^4}\right). \tag{4}$$

As discussed in § 4, the experimental results indicate that inertia effects are indeed insignificant as far as the buckling height is concerned.

Similar analysis for a plane jet from a slit with width d_1 and length D results in the following dimensionless representation:

$$\omega(d_1/g)^{\frac{1}{2}} = F_4\left(\frac{\sigma}{\gamma d_1^2}, \frac{\mu Q'}{\gamma d_1^3}, \frac{H}{d_1}, \frac{g d_1^3}{\nu^2}\right), \tag{5}$$

where Q' is the volume flow rate per unit slit length. We have assumed that the flow is one-dimensional so that $\omega(d_1/g)^{\frac{1}{2}}$ does not depend on the geometrical parameter D/d_1. This assumption is verified experimentally as discussed in § 4. Again assuming no important inertia effects as far as the buckling height is concerned, we obtain

$$\frac{H_c}{d_1} = F_5\left(\frac{\sigma}{\gamma d_1^2}, \frac{\mu Q'}{\gamma d_1^3}\right). \tag{6}$$

Experiments were conducted to establish the functional relationships indicated in (2), (4), (5) and (6).

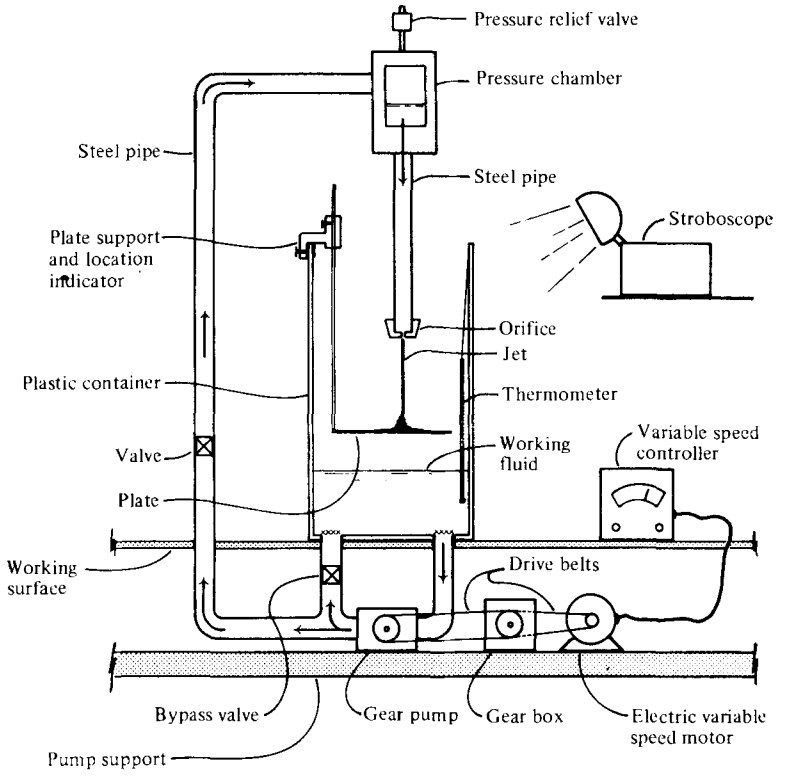

FIGURE 6. Schematic diagram of fluid-buckling apparatus.

3. Description of the experiment

The basic apparatus for the experiments, shown in figure 6, contains an orifice through which a high-viscosity fluid is pumped. The resulting fluid jet impinges on a flat plate a known distance H below the orifice, as in figure 1.

The apparatus consists of a clear plastic container with outlets in the base through which the working fluid can be drawn by the pump for circulating through the steel pipe into the pressure chamber. The fluid is then forced through the orifice at the end of the vertical steel pipe and onto the plate. It is then allowed to flow over the sides of the plate, where it collects at the bottom of the container, and then the cycle continues.

The pump is gear-type and is driven by a variable-speed electric motor. For very low flow rates through the orifice, some of the fluid can be bypassed directly back into the container without passing through the orifice.

A thermometer is incorporated for monitoring the fluid temperature so that its viscosity can be determined. A stroboscope was used for measuring the rate of coiling or folding ω of the buckled flow. The working fluid was mainly Dow Corning 200 silicone oil which was chosen because of its fairly flat viscosity–temperature curve, its availability over a wide range of very high viscosities and its clarity. Other high-viscosity fluids such as sorghum and corn syrup (which have surface tensions different from that of silicone oil) were used at times, although most of the results were obtained

with silicone oil. As shown, in part, by the linear shear stress versus rate of strain results presented by Suleiman & Munson (1981), these are Newtonian fluids.

The fluids used had viscosities ranging from 1000 centistokes (cSt) to 30000 cSt. It is to be noted that these values are three to four orders of magnitude larger than that for water, which has a kinematic viscosity of approximately 1 cSt. The surface tension of the silicone oil was approximately 22 dyn/cm, while those of the water-based sorghum and corn syrup were about 55 and 68 dyn/cm, respectively. The viscosity was measured using a calibrated capillary tube viscometer, while the surface tension was measured using a ring surface tensiometer. The seven orifice diameters used in the axisymmetric experiments ranged from 0·114 to 1·91 cm. For the plane jet, nine slits were used with $D/d_1 = 5$, 10, and 15 and D from 0·990 to 4·14 cm.

The orifice to plate distance at which buckling first begins H_c, and the resulting value of ω (see figure 1) at and beyond this point, were measured for the various orifice sizes and geometries, at different fluid flow rates Q, and at varying values of H.

The value of ω was measured with a stroboscope; the fluid flow rate Q was measured by collecting an amount of fluid over a period of time and weighing the result; and the plate to orifice distance H was read off an appropriate measuring gauge.

While the phenomenon of coiling or folding can be adequately produced by having the fluid jet impact on a surface of similar, stagnant fluid, this was avoided in favour of having it impact on a solid surface so as to reduce the possibility of bubble formation in the viscous fluid with the attendant fluid property deterioration. All efforts were made to run the experiment without bubbles in the fluid; however, for the high-viscosity fluids used, it was difficult to avoid the formation of bubbles at all times. Such occasions, however, were kept to a minimum.

4. Experimental results

As shown in figures 1–4, the stable flow ceases to exist when the plate–orifice distance reaches some critical value. The fluid column starts to oscillate, presumably as a result of the disturbance of the jet column inherent in moving the plate or from other natural disturbances. If the jet length is less than the critical length, the oscillations soon die out and the column remains stable.

If, however, the plate–orifice distance is fairly close to the critical value, the oscillations take longer and longer to die out. As the plate gets nearer and nearer to the buckling point, the oscillations become self-sustaining, and the column, or the lower parts of it, continue to oscillate at some fixed frequency ω so long as other parameters such as flow rate and plate–orifice distance remain fixed. The nature of some typical coils formed after buckling of the axisymmetrical jet can be seen in figure 2. Figure 2(*a*) shows a particularly smooth form of the coiling that is obtained under some circumstances, and figure 2(*b*) is an example of the two-dimensional folding obtained with an axisymmetric jet just before all oscillations disappear as the flow rate gets very high. The plane jet, which behaves similarly, does not coil but instead folds sinusoidally, also at a specific frequency (figure 3).

It is of interest to note that the buckling can occur independently of gravity. Figure 5 shows fluid buckling in the case of a horizontal jet of silicone oil issuing from an orifice onto the horizontal surface of a container of water. For vertical jets (all cases discussed in this paper except the example shown in figure 5) gravity is an important

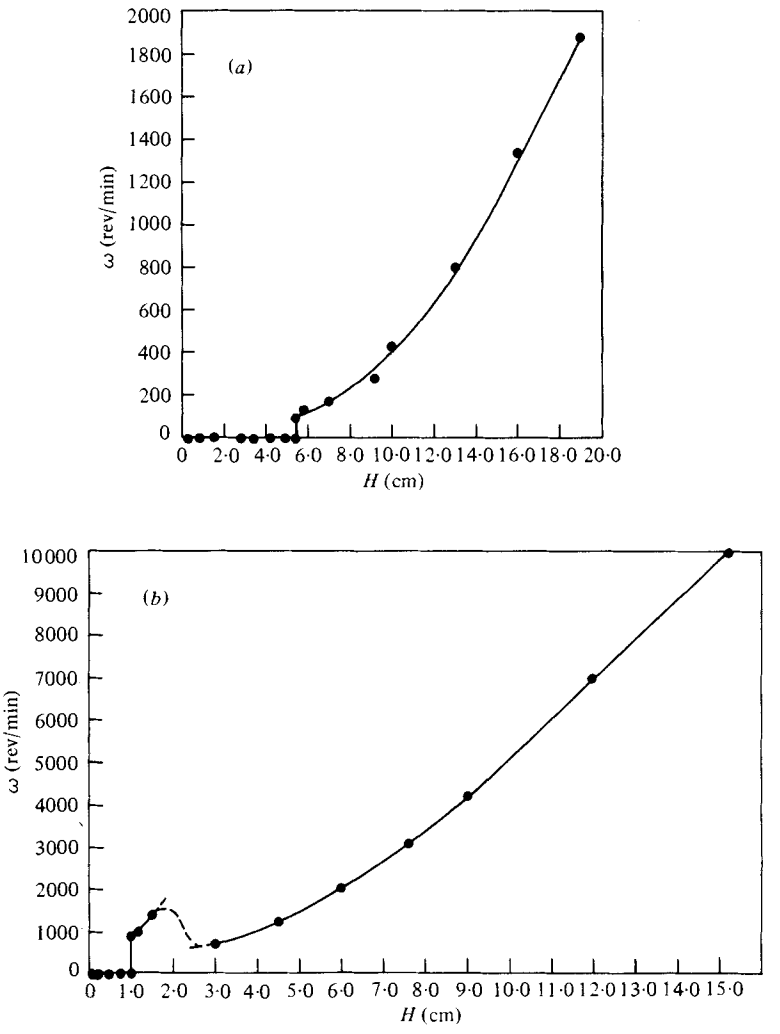

FIGURE 7. Frequency of oscillation ω as a function of jet length H, for typical axisymmetric jets. (*a*) $d = 1{\cdot}91$ cm, $Q = 9{\cdot}01$ cm^3/s, $\nu = 10000$ cSt; (*b*) $d = 0{\cdot}114$ cm, $Q = 2{\cdot}11$ cm^3/s, $\nu = 5500$ cSt.

force producing the basic stable, unbuckled jet. However, as shown by figure 5, for which gravity acts normal to the axis of the jet, gravity is not an essential ingredient for producing the buckling instability. The flow is not driven by gravity, but the jet can still buckle and oscillate in the horizontal plane.

Like its counterpart in solid mechanics, fluid buckling can occur for all types of interesting geometries. Figure 4 shows buckling for the case of a high-viscosity fluid flowing through an X-shaped slit.

Although most of the results presented are in dimensionless form, some results are presented in dimensional form in figures 7 and 8 for typical axisymmetric jets.

As indicated above, the basic flow is a pure stagnation jet flow if the plate is fairly close to the orifice. This type of flow is maintained until the critical distance is reached. It is at this critical distance H_c that the first spontaneous oscillations are observed. They start from the axisymmetric jet as purely sinusoidal two-dimensional waves,

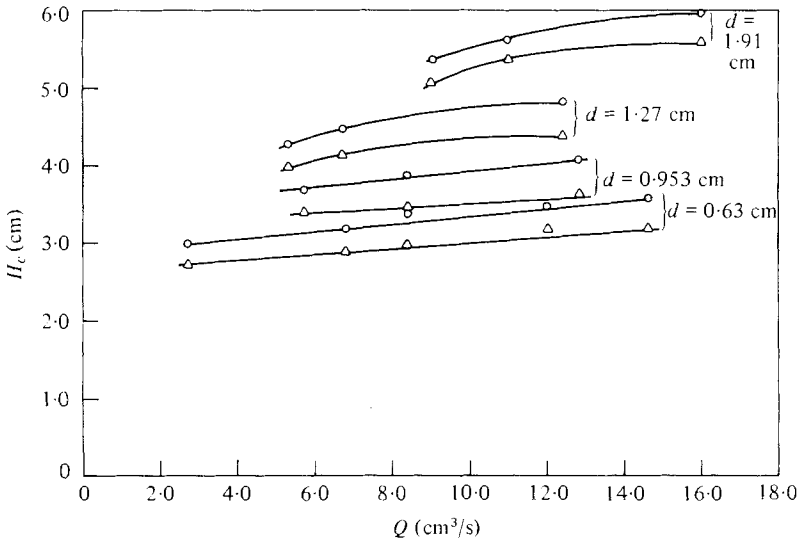

FIGURE 8. Buckling height H_c as a function of flow rate Q for typical axisymmetric jets. ν = 10000 cSt. ○, plate moving away from orifice; △, plate moving toward orifice.

folding rather than coiling, but quickly turn into helical coils of fixed frequency. The oscillations may also start in the form of coiling. The direction of rotation of the coils may be either clockwise or anti-clockwise with no preferred direction discernible. The plane jet is always observed in the folding mode when it becomes unstable.

The frequency of the coiling generally tends to increase with plate distance H, although there is a short distance over which in some instances (small jet diameter, high flow rate) the frequency decreases with H before increasing again (figure 7). In this region, the rate and type of spin for the axisymmetric jet seems rather random with a mixture of two-dimensional sinusoidal waves and helical coils of apparently different frequencies existing simultaneously.

The buckling height for axisymmetric jets generally shows a slight increase with flow rate and a fairly significant one with increases in orifice diameter (figure 8). A hysteresis effect is observed, with the buckling height being different for the two cases of plate moving away from the orifice (buckling begins) or moving towards it (buckling stops). In the latter case, the spinning continues for a short distance past the original point of buckling, resulting in consistently lower values of H_c. Except for the data of figure 8, all the data presented in this paper are based on measurements obtained with the plate moving away from the orifice (from a stable to an unstable configuration).

This general behaviour is maintained with increasing fluid flow rate until at values of the Reynolds number (based on orifice diameter and fluid velocity at orifice, $Re = 4Q/\pi\nu d$) that are of the order of 0·1–1·0. In this range the helical oscillations for the axisymmetric jet begin to disappear and are replaced by two-dimensional sinusoidal folding of the jet column (figure 2*b*). The plane jet is always observed in the folding mode. Further increases in the flow rate corresponding to Reynolds numbers Re of around 1·2 for the axisymmetric jet cause the oscillations to disappear altogether. This is a critical Reynolds number beyond which the jet returns to stagnation flow at all plate distances from the jet exit. For the plane jet, the critical Reynolds number

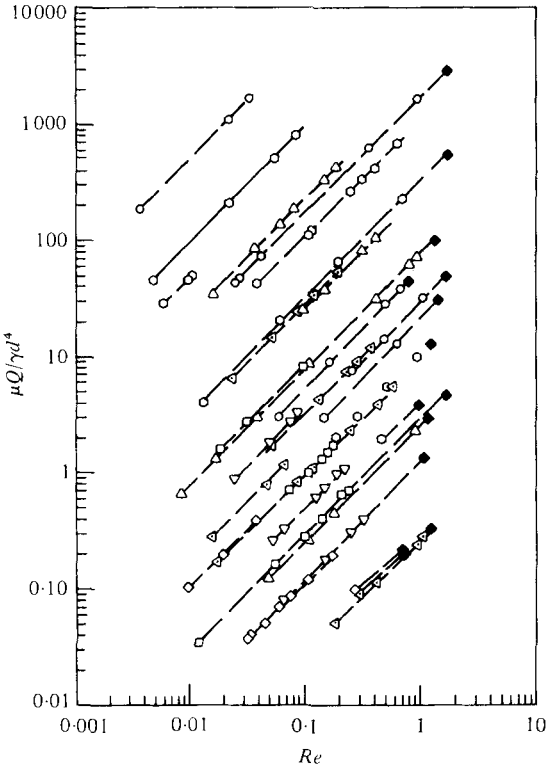

FIGURE 9. Range of parameters for which jet will buckle. Solid symbols represent upper limit of Reynolds number beyond which jet will not buckle. Symbols show different values of $\sigma/\gamma d^2$. ○, 1·77; ●, 0·59; △, 0·23; ◁, $5{\cdot}64 \times 10^{-2}$; □, $2{\cdot}54 \times 10^{-2}$; ▽, $1{\cdot}43 \times 10^{-2}$; ◇, $6{\cdot}33 \times 10^{-3}$.

based on d_1 (slit width) averages about 0·56. Apparently, this Reynolds-number limitation is the reason that jets of low viscosity, such as water, are not observed to buckle.

Owing to limitations on the size of our equipment, the maximum plate distance to orifice diameter ratio H/d used was around 150. Presumably, as this ratio gets larger and larger, surface tension would begin to play a significant role resulting in the well-studied problem of jet breakup into drops (McCarthy & Molloy 1974). However, with the flow rates, viscosity, and distances used in this experiment, jet breakup was not observed.

The coiling or folding frequency may become very large in some instances. For example, frequencies as high as 167 Hz were observed for the axisymmetric jet, with a 5500 cSt silicone oil and an orifice diameter of 0·114 cm (0·045 in) at a distance equivalent to 133 orifice diameters from the exit (figure 7). Frequencies of similar magnitude were observed for the smallest plane jets.

The height and character of the coiled fluid varies considerably with jet characteristics and plate distance. It ought to be pointed out that, while this study required a flat plate to facilitate the measurement of distance, the coiling or folding effect can be produced by any object that is intruded into the mainstream of the jet if its distance from the orifice is greater than the critical distance needed for buckling.

Some of the dimensionless results of the jet buckling study are shown in figures 9–

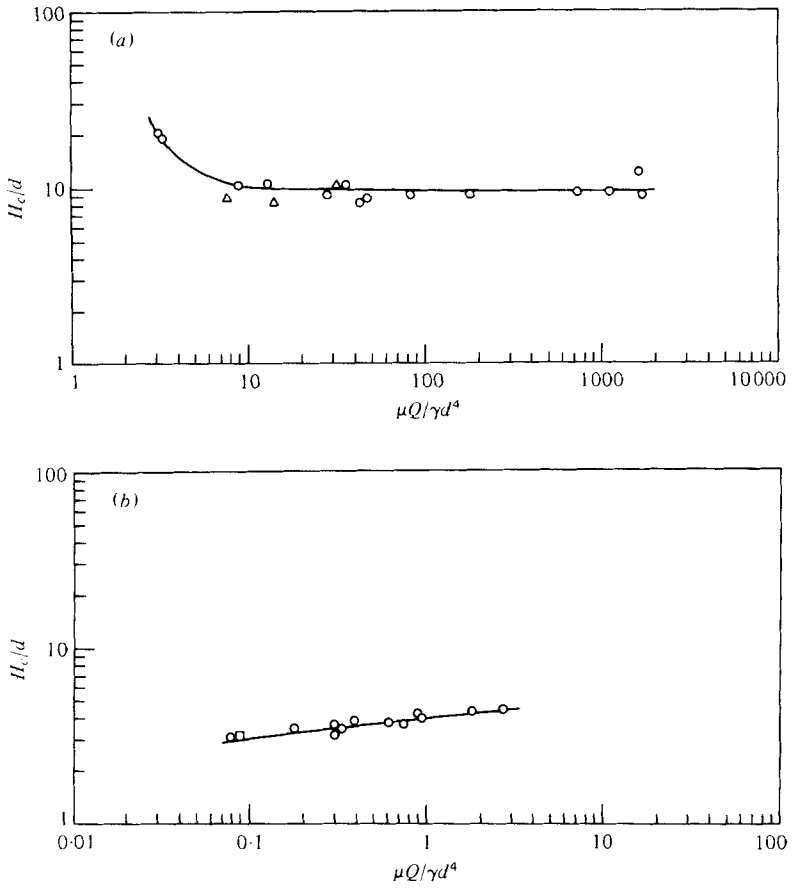

FIGURE 10. Axisymmetric jet non-dimensional buckling height as a function of viscous, gravity and surface tension effects. (*a*) ○, silicone oil, $\sigma/\gamma d^2 = 1{\cdot}77$; △, corn syrup, $\sigma/\gamma d^2 = 1{\cdot}15$; (*b*) ○, silicone oil, $\sigma/\gamma d^2 = 1{\cdot}15 \times 10^{-2}$; □, sorghum, $\sigma/\gamma d^2 = 1{\cdot}43 \times 10^{-2}$.

13 and discussed below. The purpose of these graphs is to illustrate the functional relationship among the various dimensionless quantities identified in § 2.

Figure 9 is constructed specifically to indicate the range of Reynolds numbers over which experiments could be carried out in order to emphasize the Reynolds-number effect at higher flow rates. The Reynolds number is based on the orifice fluid velocity and the orifice diameter. Thus, this parameter is different from the one involving inertia used in § 2 (gd^3/ν^2) which was designed so as to reflect more local velocity effects by using fluid acceleration due to gravity.

There is, of course, a lower limit on the flow rate (Reynolds number Re equal to $4Q/\pi\nu d$) for the experiment. This has to do with the need for some minimum flow rate to ensure that a jet is produced (Zaik 1979). If the flow rate is too small, the fluid either drips from the orifice (for small diameter jets) or peels away from the wall and does not fill the orifice (for large diameter jets). Such conditions tend to occur along the left side and bottom of the 'thumbprint' region of the ($\mu Q/\gamma d^4$, $4Q/\pi\nu d$) plane shown in figure 9.

There is also an upper limit on the flow rate (Reynolds number) for the experiment. Figure 9 emphasizes the fact that the point beyond which the jet does not buckle,

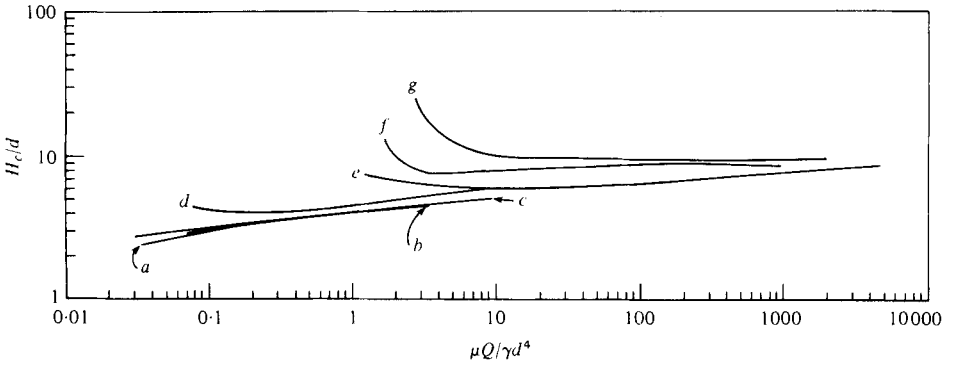

FIGURE 11. Axisymmetric jet non-dimensional buckling height for a wide range of the surface tension parameter $\sigma/\gamma d^2$, the values being (*a*) $6{\cdot}33 \times 10^{-3}$; (*b*) $1{\cdot}43 \times 10^{-2}$; (*c*) $2{\cdot}54 \times 10^{-2}$; (*d*) $5{\cdot}64 \times 10^{-2}$; (*e*) 0·23; (*f*) 0·59; (*g*) 1·77.

regardless of the value of H/d, coincides roughly with the point at which the Reynolds number is about 1·0. For the axisymmetric jet the average value of this critical Reynolds number was actually 1·2. All the other points represent data points in the $(\mu Q/\gamma d^4, 4Q/\pi\nu d)$ plane for which the critical height H_c was determined. This figure establishes the approximate upper and lower Reynolds number boundaries within which the experiment could be performed.

As indicated functionally in (4), the dimensionless buckling height, H_c/d, is expected to be dependent on the dimensionless surface tension parameter $\sigma/\gamma d^2$, and the dimensionless viscosity parameter $\mu Q/\gamma d^4$. Physically, these two parameters are the ratio of surface tension to gravitational forces and the ratio of viscous to gravitational forces, respectively. The experimental data indicated that because of the high viscosities and low speeds involved, inertia effects were insignificant. The exception to this was the existence of a critical Reynolds number (mentioned in the previous paragraph) above which the jet would not buckle for any H/d. For flows with the same value of $\mu Q/\gamma d^4$ but with Reynolds numbers less than this critical value, the value of H_c/d was found to be independent of the Reynolds numbers.

The following general characteristics can be inferred from the results presented in figures 10 and 11. Figure 10 shows typical results for two extreme values of the surface tension parameter, and figure 11 is a composite of several curves. The experimental data points were excluded from figure 11 for better clarity. The surface tension parameter $\sigma/\gamma d^2$ was varied by using different diameter orifices d, and, in some instances, by using different fluids (silicone oil, corn syrup, or sorghum). For a constant value of $\sigma/\gamma d^2$, the parameter $\mu Q/\gamma d^4$ was varied by varying the flow rate Q.

Over a range of 0·01–10000 for the $\mu Q/\gamma d^4$ parameter and a range of 0·0063–1·77 for the $\sigma/\gamma d^2$ parameter, H_c/d varies between 2 and 30. Thus, H_c/d varies over only one order of magnitude while $\mu Q/\gamma d^4$ varies over six orders of magnitude and $\sigma/\gamma d^2$ varies over three orders of magnitude. Although the dependence of H_c/d on $\sigma/\gamma d^2$ and $\mu Q/\gamma d^4$ is quite strong over portions of the parameter space, it is, in general, rather weak over most of the range of parameters tested.

It is obvious that surface tension can make a significant change in the non-dimensional buckling height, especially at very low flow rates. This is particularly so if the orifice diameter is quite small and can be seen by the upturn at the left end of the

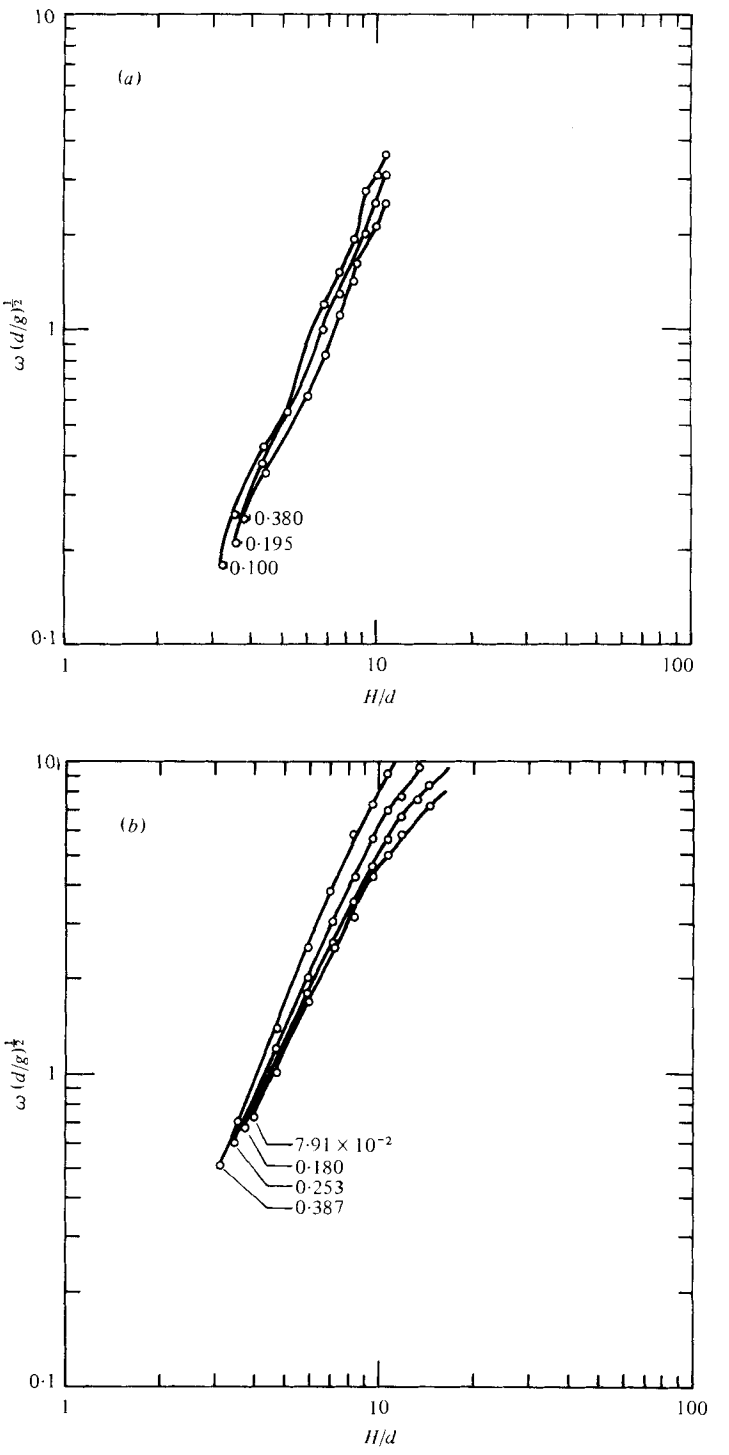

FIGURE 12. Rate of spin of a buckled axisymmetric jet as a function of flow variables. Each curve is labelled with the value of $\mu Q/\gamma d^4$. Other parameters are (*a*) $\sigma/\gamma d^2 = 6{\cdot}33 \times 10^{-3}$ and $gd^3/\nu^2 = 7{\cdot}59 \times 10^{-2}$; (*b*) $\sigma/\gamma d^2 = 1{\cdot}43 \times 10^{-2}$ and $gd^3/\nu^2 = 0{\cdot}66$; (*c*) $\sigma/\gamma d^2 = 2{\cdot}54 \times 10^{-2}$ and $gd^3/\nu^2 = 8{\cdot}48 \times 10^{-2}$; (*d*) $\sigma/\gamma d^2 = 5{\cdot}64 \times 10^{-2}$ and $gd^3/\nu^2 = 2{\cdot}85 \times 10^{-3}$; (*e*) $\sigma/\gamma d^2 = 0{\cdot}59$ and $gd^3/\nu^2 = 2{\cdot}5 \times 10^{-3}$; (*f*) $\sigma/\gamma d^2 = 0{\cdot}59$ and $gd^3/\nu^2 = 8{\cdot}45 \times 10^{-5}$.

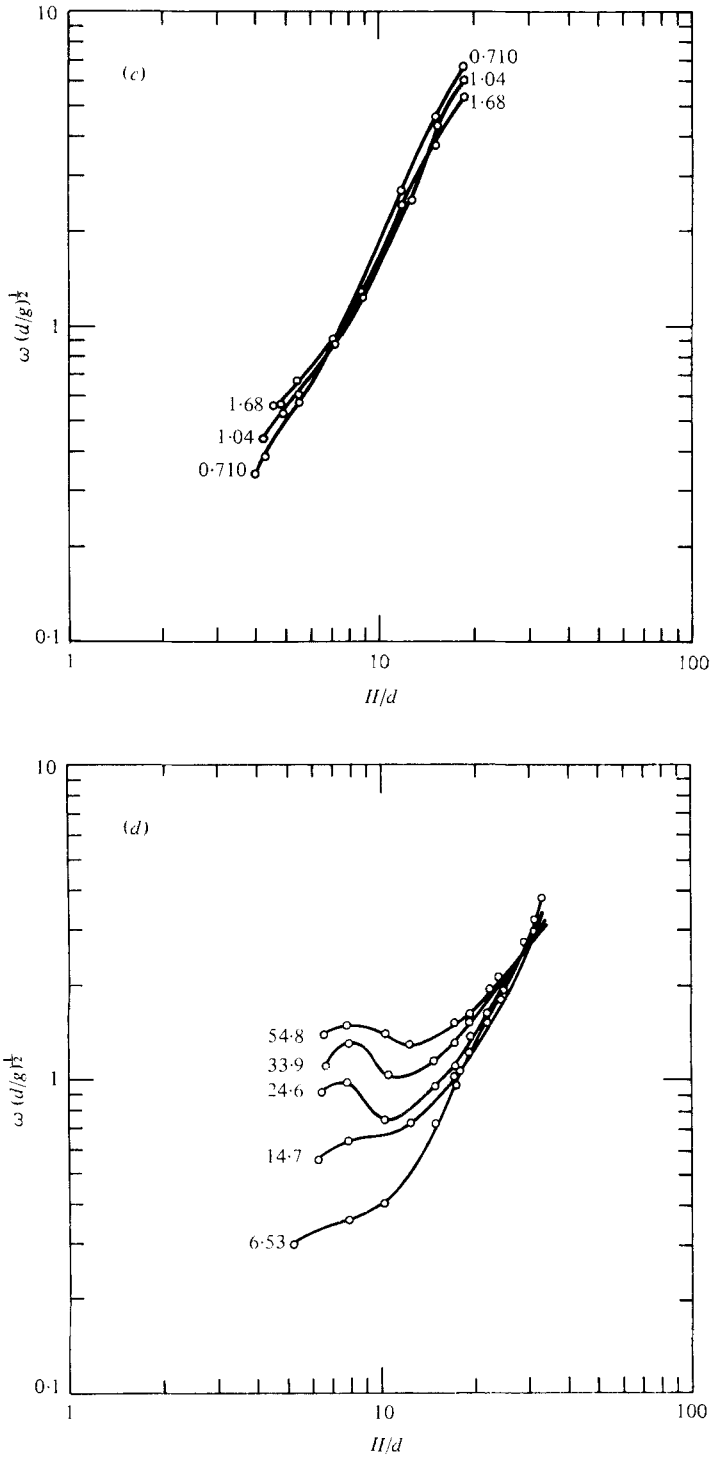

FIGURE 12*c*, *d*. For legend see p. 234.

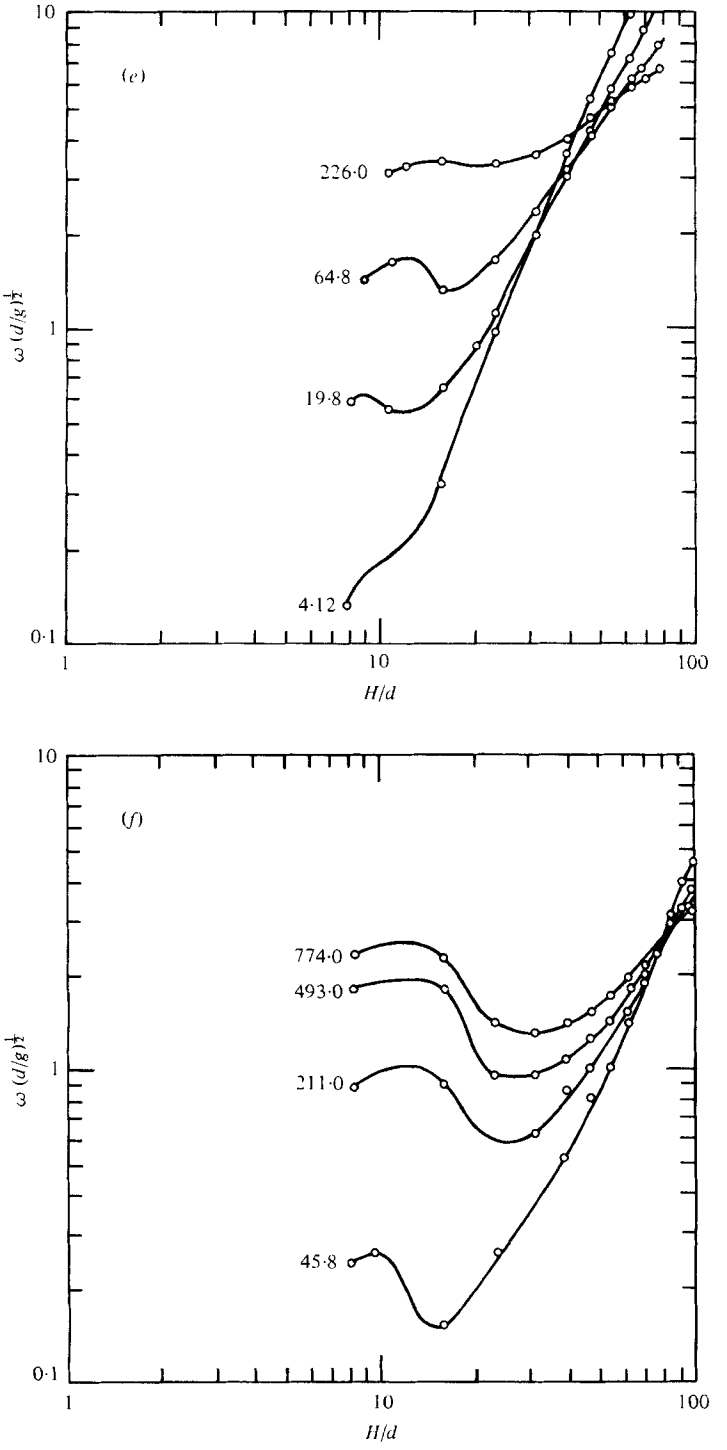

FIGURE 12*e*, *f*. For legend see p. 234.

large $\sigma/\gamma d^2$ curve of figure 11. On the contrary, at larger diameters (lower values of $\sigma/\gamma d^2$) the effect of surface tension is almost negligible to the point where there is hardly any difference in H_c/d for various values of $\sigma/\gamma d^2$.

As indicated by (2), the non-dimensional coiling or spin rate of a buckled axisymmetric jet is expected to be a function of the surface tension, viscosity, and inertia parameters and the length to diameter ratio H/d of the jet. Typical results for a fairly wide range of parameters are shown in figure 12. Additional parameter values are covered in the work by Cruickshank (1980).

The data for the curves of figure 12 were obtained as follows. The surface tension parameter $\sigma/\gamma d^2$ was fixed for a given fluid and orifice diameter. Curves of $\omega(d/g)^{\frac{1}{2}}$ as a function of H/d for given $\mu Q/\gamma d^4$ were obtained by adjusting the flow rate to give the desired value of $\mu Q/\gamma d^4$. The orifice–plate distance H was varied and the frequency of the coiling ω was measured with a strobe light. Various combinations of flow rate, orifice diameter and fluid properties were used. Each combination produced one curve in figure 12.

As discussed earlier, the fluid first buckles at some critical plate-to-orifice distance and, as a consequence of this instability, the fluid stream, or parts of it, begin to oscillate. Generally, the oscillations are helical from the start, but some jets (in most cases for the large-diameter jets) have been observed to swing back and forth more like a pendulum. In any case, the only mode observed as the plate is moved further away from the buckling point is the helical mode. There is, however, a tendency under some circumstances for the return of the oscillations to a mix of helical and folding patterns at some plate location a few diameters downstream of the buckling point. This rather random pattern does not occur all the time or with all flow conditions but is generally observed for small-diameter, low flow rates, and high surface tension and viscosities. When it occurs, it tends to coincide with the turning points on the graphs of figure 12. In figure 7, for example, it was observed in the region marked by the dashed lines. It was not a very frequent occurrence and, furthermore, it was difficult to measure the frequencies because of the randomness of the oscillations.

As the plate is moved further downstream of the orifice, the oscillations return in all cases, for the axisymmetric jet, to the helical mode. There appears to be a general pattern to the behaviour of these oscillations, and the dimensional plot of figure 7 clearly shows that, aside from the pecularities observed at lower values of H, the spin rate generally increases with orifice-to-plate distance. The results shown in figure 12 indicate in several instances a 'cross-over' effect such that, for any two different values of $\mu Q/\gamma d^4$, the spin rate is higher for the larger $\mu Q/\gamma d^4$ at low values of H/d and lower at higher values of H/d. However, the sensitivity of the spin rate to fluid flow rate at fairly large values of H/d does not appear to be very significant.

Decreasing the viscosity generally tends to increase the region over which a linear relationship exists between $\omega(d/g)^{\frac{1}{2}}$ and H/d and de-emphasizes the initial peaks and valleys found at larger values of gd^3/ν^2. It is suspected that low viscosities generally would cause a more nearly one-dimensional (axial) flow pattern, thus resulting in a pattern of behaviour that is more consistently uniform than those that would be observed in a flow that could be at times two-dimensional (axial and radial) and, thus, is forced to display either character depending upon the geometrical and flow condition to which it is subjected.

The argument is further supported by the behaviour of the graphs when surface

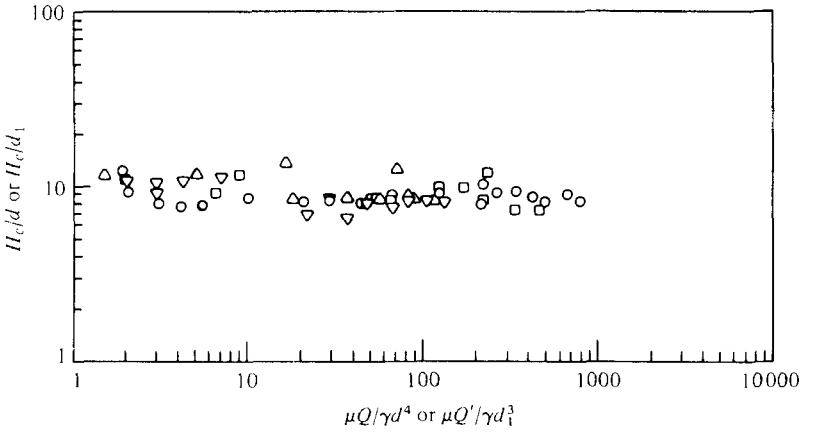

FIGURE 13. Buckling height for plane and axisymmetric jets for a given value of the surface tension parameter. $\sigma/\gamma d^2 = \sigma/\gamma d_1^2 = 0{\cdot}59$. ○, Axisymmetric jets. Plane jets: □, $D/d_1 = 5{\cdot}0$; ▽, $D/d_1 = 10{\cdot}0$; △, $D/d_1 = 15{\cdot}0$.

tension effects are taken into account. The same effects described earlier (longer linear portions of the graphs) are observed as the effect of surface tension is reduced. Thus, it can be postulated that high viscous and surface tension effects generally would emphasize the two-dimensional aspects of the flow and would result in less uniform behaviour of the coiling parameters.

The buckling behaviour for plane jets is generally similar to that of the axisymmetric jet and the same general comments hold for the plane jet as well. Additional data for both plane and axisymmetric jets can be found in the work by Cruickshank (1980).

Figure 13 is a composite of the buckling heights for data obtained from both the axisymmetric and plane jet experiments for one surface tension parameter, $\sigma/\gamma d_1^2 = 0{\cdot}59$. Clearly, it indicates that the buckling height is not significantly affected by flow geometry. Different slit length to width ratios D/d_1 are involved. For the axisymmetric jet, D/d_1 may be deemed to be equal to 1·0. The lack of sensitivity to this ratio is noted.

In general, the plane jet buckles by folding and there is none of the mixed oscillations (coiling and folding) discussed above for the axisymmetric jet. If, however, the plane jet is allowed to become small enough in terms of its width and length (either because D/d_1 is nearly equal to one, or if the flow rate is small enough or the plane is far enough away) the folding may stop and coiling may begin.

Minimum flow rates were maintained to ensure that the folding behaviour was obtained throughout the range of our experiments. As with the axisymmetric jet, all oscillations stopped at some Reynolds number (based on orifice fluid velocity and orifice width). For the experiments conducted, the critical Reynolds number averaged 0·56. Above this value, the flow returned to the stable stagnation flow similar to that shown in figure 3(*a*).

5. Conclusions

A jet of a very viscous fluid flowing against a flat surface may become unstable and buckle in a fashion somewhat analogous to the buckling of a long slender solid column. There is a critical length-to-diameter ratio H_c/d at which either a plane jet or an axisymmetric jet will buckle. They are both stable to external disturbances at plate-to-orifice distances less than this value. Surface tension appears to be the most significant parameter affecting this critical length, although there is some dependence on other flow and fluid variables. High values of surface tension tend to increase the critical height. For a given value of the surface tension parameter, the buckling height appears to be independent of jet geometry. That is, H_c/d is essentially the same for plane jets of various aspect ratios as it is for axisymmetric jets.

The frequency of the oscillations that result when the jet length is greater than the critical value generally increases with an increase in the orifice-to-plate distance. In some cases, however, there is an initial region in which the frequency decreases with this distance.

The buckling instability described here is a low-Reynolds-number phenomenon. If the Reynolds number of the jet at the orifice is large enough (approximately 1·2 for the axisymmetric jet and 0·56 for the plane jet), the jet will not buckle for any length-to-diameter ratio. Perhaps in these cases inertia effects are large enough to overpower the viscous compressive normal stress effects, not allowing the jet to buckle.

Thus there are two critical parameters associated with the buckling of a viscous jet as described here. First, the length-to-diameter ratio must be large enough in order for the jet to become unstable. Second, the Reynolds number must be small enough to ensure that inertia effects are not important. This is in contrast to the more common situations in which instabilities occur when the Reynolds number becomes sufficiently large.

The support of the Engineering Research Institute of Iowa State University through funds provided by the National Science Foundation, Grant Number ENG78-19373, has been appreciated.

REFERENCES

CRUICKSHANK, J. O. 1980 Viscous fluid buckling: A theoretical and experimental analysis with extensions to general fluid stability. Ph.D. dissertation, Iowa State University, Ames, Iowa.

LIENHARD, J. H. 1968 Capillary action in small jets impinging on liquid surfaces. *J. Basic Eng.* (Trans. of ASME), pp. 137–138.

MCCARTHY, M. J. & MOLLOY, N. A. 1974 Review of stability of liquid jets and the influence of nozzle design. *Chem. Eng. J.* **7**, 1–20.

SULEIMAN, S. M. & MUNSON, B. R. 1981 Buckling of a thin sheet of a viscous fluid. *Phys. Fluids*, **24**, 1–5.

TAYLOR, G. I. 1968 Instability of jets, threads, and sheets of viscous fluids. *Proc. Int. Congr. Appl. Mech.* Berlin: Springer-Verlag.

ZAIK, M. 1979 Dynamics of liquid films and thin jets. *SIAM J. Appl. Math.* **32**, 276–289.